Sensors and Actuators B 244 (2017) 785–795

Contents lists available at ScienceDirect

Sensors and Actuators B: Chemical

journal homepage: www.elsevier.com/locate/snb

A novel electrochemical imprinted sensor for acetylsalicylic acid based on polypyrrole, sol-gel and SiO_2@Au core-shell nanoparticles

Behjat Deiminiat, Iman Razavipanah, Gholam Hossein Rounaghi*, Mohammad Hossein Arbab-Zavar

Department of Chemistry, Faculty of Sciences, Ferdowsi University of Mashhad, Mashhad, Iran

ARTICLE INFO

Article history:
Received 7 October 2016
Received in revised form
19 December 2016
Accepted 8 January 2017
Available online 13 January 2017

Keywords:
Acetylsalicylic acid
Molecularly imprinted polymer
Polypyrrole
Sol-gel
Core-Shell

ABSTRACT

A new nanocomposite imprinted electrochemical sensor was developed for sensitive and selective determination of acetylsalicylic acid (ASA), based on a gold electrode modified with one-step electropolymerization of the molecularly imprinted polymer (MIP) composed from polypyrrole (ppy), sol-gel, Silica@Gold core-Shell nanoparticles (SiO_2@AuNPs) and acetylsalicylic acid. SiO_2@AuNPs were introduced into the polymer matrix for the enhancement of electrical response of $[Fe(CN)_6]^{3-}/[Fe(CN)_6]^{4-}$ redox pair which was used as an electrochemical active probe. The SiO_2@AuNPs, were synthesized chemically by using a modified Stober method and they were characterized by UV–Vis spectrophotometry, Fourier transform infrared (FT-IR) spectrometry, X-ray diffraction (XRD), scanning electron microscopy (SEM) and transmission electron microscopy (TEM). Under the optimized experimental conditions, two linear concentration ranges from 1.0 to 10.0 nM and 10.0–100.0 nM with a limit of detection (LOD) of 0.2 nM was obtained. The effects of interfering species on the determination of ASA were investigated and it was found that the proposed sensor has a high recognition capacity towards the ASA in the presence of interfering species in solutions. Moreover, the reproducibility, repeatability and stability of the imprinted sensor were all found to be satisfactory. Finally, the modified electrode was successfully applied for determination of ASA in tablet and urine samples.

1. Introduction

Acetylsalicylic acid (ASA), commonly known as aspirin, is one of the most important nonsteroidal anti-inflammatory, analgesic and antipyretic drugs in the world. It is widely used to relieve minor aches, pains and reduce fever and is also great effective in treating the antithrombotic, coronary heart disease, preventing colon cancer and pregnancy induced pre-eclampsy [1,2]. Such widespread use of aspirin has resulted in problems of overdose especially in persons suffering from chronic inflammatory diseases, who take this drug habitually [3]. Various methods have been proposed for the determination of ASA and its metabolites such as high-performance liquid chromatography (HPLC) [4,5], gas chromatography [6], Raman spectroscopy [7], ultraviolet spectrophotometry and spectrofluorimetry [8,9]. These methods are usually expensive and complicated and long time is required for pretreatment of the samples prior to their determination. Electrochemical methods including voltammetric techniques have also been developed for the detection of ASA using chemically modified electrodes [10,11]. Since the electrochemical activity of ASA is weak and it oxidizes at high potential, there are a few reports about its measurement using electrochemical methods. Accordingly, it remains a great challenge to design a rapid, inexpensive but sensitive and selective method to determine the concentration of ASA in biological fluids.

Recently, due to high selectivity, chemical stability, low cost and easy preparation, the molecular imprinted polymers (MIPs) have been extensively employed in various fields including solid-phase extraction, chromatography and construction of chemical sensors [12–15]. The high specificity and affinity of molecular imprinted polymers toward the template molecules, make them ideal candidates as recognition elements for construction of chemical sensors. Until now, many MIP based electrochemical sensors with different mechanisms have been reported [16–18]. Although the MIPs are used as selective components for development of electrochemical sensors, the shortcomings such as slow diffusion of the analytes across the MIP film and low sensitivity still exist in their applications [19].

* Corresponding author.
E-mail addresses: ghrounaghi@yahoo.com, ronaghi@um.ac.ir (G.H. Rounaghi).

http://dx.doi.org/10.1016/j.snb.2017.01.059
0925-4005/

Sol-gel imprinting technology is a promising way to improve the performance of MIP film on the surface of the electrodes. Briefly, a rigid three dimensional silicate network with excellent permeability and uniformly porous structure is formed around a template via non-covalently/covalently interaction between functional monomers and the template during the sol-gel process [20,21]. Electrochemical deposition is a simple and effective method for the deposition of an uniform sol-gel MIP film with good adherence to the support surface. Moreover, the thickness of the deposited layer can be easily controlled by varying the amount of circulated charge [19]. However, the low electrical conductivity of the sol-gel coatings is undoubtedly a main drawback. In order to improve the electrical or electrochemical properties of the sol–gel MIP based sensors; the most effective way is the use of conducting polymers and nanomaterials.

Recently, conducting polymer modified electrodes have received considerable attention due to their good stability, reproducibility, homogeneity in electrodeposition, thickness controllability, strong adherence to the electrode surfaces and ease of the chemical substitution to modify their properties [22]. Polypyrrole is one of the most frequently used conducting polymers in design of sensors and biosensors, because it has significant electrical conductivity, good biocompatibility and facile polymerization compared to the other conducting polymers [23,24].

Metal nanoshells are a novel class of hybrid nanoparticles (NPs) consisting of a dielectric core covered by a thin metallic shell which is typically gold. Silica has been considered as one of the most ideal core materials because it is highly stable, chemically inert and biocompatible. Furthermore, the methods for functionalization of the surface of silica are well known and the colloidal silica particles can be synthesized with reproducibly spherical shapes and narrow size distributions [25]. Among all kinds of metal nanoparticles, gold nanoparticles (AuNPs) have found many applications in electrochemical and biological researches for their unique physical and chemical features such as electrical, optical and thermal properties [26,27]. The high surface-to-volume ratio, makes the gold nanoparticles a competitive candidate as shell for novel nanosized composites. The core-shell nanoparticles have high effective surface area and because of their unique structure and fascinating physical, chemical and mechanical properties, they are a promising material for sensors application [28–30]. The incorporation of SiO_2@AuNPs, polypyrrole and sol-gel technology, leads to the preparation of a new nanocomposite that possess the advantages of all aforementioned materials.

In this paper, we propose a new method to enhance the electron transfer from sol-gel MIP layer to the electrode surface via entrapment of conducting polymers and metal nanoshells within sol-gel network (Fig. 1). To our knowledge, this is the first work describing the synthesis of SiO_2@AuNPs and use of polypyrrole, sol-gel, and SiO_2@AuNPs hybrid nanocomposite as an electrochemical imprinted sensor. The function of the SiO_2@AuNPs and the performance of the imprinted film were investigated by electrochemical methods in detail. Moreover, the constructed sensor was applied for determination of ASA in real samples.

2. Experimental

2.1. Chemicals

Tetraethoxysilane (TEOS), phenyltriethoxysilane (PTEOS), trifluoroaceticacid (TFA) and tetrakis (hydroxymethyl) phosphonium chloride (THPC) were purchased from Merck (Darmstadt, Germany). Pyrrole (Merck) was purified by distillation and stored in a dark bottle in a refrigerator before use. 3-aminopropyltriethoxysilane (APTES) and hydrogen tetrachloroaurate trihydrate ($HAuCl_4{\cdot}3H_2O$) were obtained from Sigma-Aldrich (USA). Lithium perchlorate was purchased from Acros (New Jersey, USA). Acetylsalicylic acid was supplied from Temad Pharmaceutical Co. (Mashhad, Iran). All of the solvents and the other chemical reagents used in this study were of analytical grade and were obtained from Merck (Darmstadt, Germany). High purity nitrogen (99.999%, Sabalan Gas Company, Iran) was used for deaeration of the solutions.

2.2. Instrumentation

Cyclic voltammetry (CV) and square wave voltammetry (SWV) measurements were carried out using an Autolab PGSTAT 101 electrochemical workstation (Metrohm Autolab, Utrecht, The Netherlands) managed by NOVA software. Gill AC potentioastate (ACM instruments) was applied for the electrochemical impedance spectroscopic measurements. All electrochemical experiments were performed with a conventional three-electrode cell, consisting of a bare or modified gold electrode (Au electrode, 2 mm in diameter, Azar Electrode Co., Urmia, Iran), as the working electrode, an Ag/AgCl electrode as the reference electrode and a platinum wire as the auxiliary electrode. The pH of solutions was measured on a 827 Metrohm pH meter (Switzerland). Scanning electron micrographs were obtained using a LEO 1450VP scanning electron microscope (SEM, Germany). A LEO 912 AB transmission electron microscope (TEM) was employed for core-shell structure verification. X-ray diffraction (XRD) analysis was carried out with an X-ray diffractometer (Philips analytical X-ray). The Fourier transform infrared (FT-IR) spectra were obtained by an AVATAR-370 Fourier transform infrared spectrometer. The UV–Vis spectra were recorded by an Agilent 8453 UV/Vis spectrophotometer.

2.3. Synthesis of silica core and surface functionalization

Silica nanoparticles (NPs) were synthesized by employing a modified Stober method [31] which involves the hydrolysis and condensation of tetraethylorthosilicate (TEOS), by a sol-gel process. Briefly, 1 mL of TEOS was added to 50.0 mL of absolute ethanol. The mixture was stirred vigorously, followed by the dropwise addition of 4.0 mL of ammonia (32% NH_3 as NH_4OH assay). The resultant SiO_2 NPs were then functionalized with amine group by heating the mixture of 0.2 gr SiO_2 NPs and 3-aminopropyltriethoxysilane (APTES) (12 mM) in volume ratio of 3:7 in ethanol (125 mL) under vigorous stirring at 76 °C for 4 h. Then, the amine grafted silica nanoparticles were cooled to room temperature and washed with HPLC grade water at least three times through centrifugation and then redispersed in HPLC grade water to remove the residual reactants before drying it by a vacuum pump.

2.4. Synthesis of SiO_2@Au core-shell nanoparticles

SiO_2@AuNPs were synthesized by the following three step procedure. The first step involves the formation of the colloidal gold NPs. For this purpose, 0.5 mL of 1 M NaOH and 1 mL of THPC solution were added to 50 mL of HPLC grade water. The mixture was stirred for 5 min under a strong vortex in a reaction flask. Then, 1.0 mL of 1% $HAuCl_4$ aqueous solution was added to the stirred solution, and it was stirred further for 30 min. At this time, the color of the solution changed quickly from colorless to dark reddish yellow and the resulting solution was stored at 4 °C for at least 3 days before further use. For attachment the colloidal gold NPs to APTES functionalized silica cores, 0.1 gr of —NH functionalized SiO_2 NPs was dispersed in 2 mL ethanol under sonication. Then, 15 mL of gold colloid solution was added to the above mixture and it was gently stirred for 3 h and then centrifuged at 10000 rpm. A violet-colored sediment was

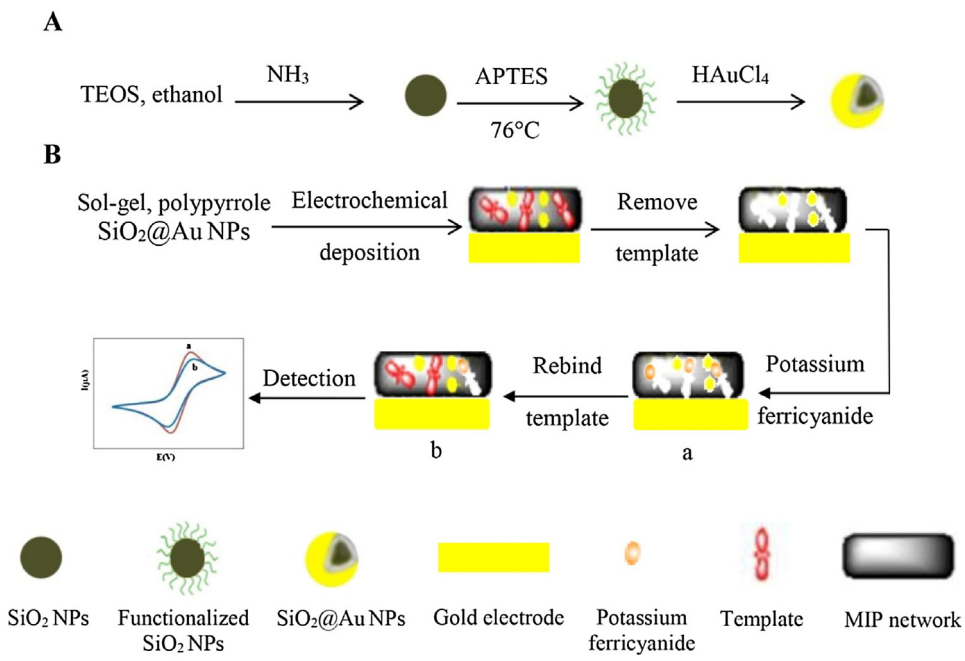

Fig. 1. Schematic representation of the proposed approach for the A) synthesize of SiO_2@AuNPs and B) fabrication of imprinted sensor.

observed at the bottom of the tube which was redispersed in 5 mL HPLC grade water by sonication and centrifuged for at least 3 times.

In order to grow the gold nanoshells on the Au/APTES/SiO_2 NPs, 2.5 mg of potassium carbonate, as a strong reducing agent, was dissolved in 10 mL of HPLC grade water by stirring for 3 min. Then, 0.2 mL of 1% $HAuCl_4$ solution was added while the solution was stirred vigorously. During this period, the color of the solution changed from yellow to colorless. Thereafter, we added 1 mL of the solution containing the Au/APTES/SiO_2 NPs to the colorless solution. Finally, 15 μL of formaldehyde was injected slowly to the solution and it was stirred for 30 min at 65 °C. At this time, the color of the solution became dark violet which reveals the formation of gold nanoshells. After cooling the solution to room temperature, it was centrifuged and redispersed in HPLC grade water to remove residual reactants. At the last step, the solid products were dried for 24 h under vacuum at 60 °C to obtain SiO_2@AuNPs as a violet powder.

2.5. Fabrication of polypyrrole/sol-gel/SiO_2@AuNPs MIP/Au electrode

Prior to electropolymerization, the surface of the gold electrode was polished carefully with 0.3 and 0.05 μm alumina slurry. The polished surface was then sonicated in double distilled water and ethanol for 5 min, respectively. Then it was subjected to sweep the potential cyclically between −0.2 and 1.5 V in 1.0 M H_2SO_4 solution until a stable cyclic voltammogram was obtained. To prepare the ASA-imprinted sol solution, a mixture of 75 μL PTEOS, 75 μL TEOS, 700 μL water, 1100 μL ethanol, 10 μL TFA and ASA (1.0 mM) was stirred for 2 h to obtain a homogeneous sol at room temperature. Then, 50 μL of pyrrole solution, 5.0 mg of lithium perchlorate and 30 μL of 0.1% SiO_2@AuNPs core-shell solution were added to the mixture. The resulting solution was sonicated for 10 min. This solution was used for electropolymerization of the imprinted sol-gel film (polypyrrole/sol-gel/SiO_2@Au NPs MIP/Au electrode) and a solution without ASA was used for the preparation of the non-imprinted sol-gel film. Cyclic voltammetry was applied for electrodeposition of the imprinted sol-gel film on the surface of pretreated electrode in the potential range of −0.8 V to +0.8 V in 5 cycles and at a scan rate of 50 mV s^{-1}. After electrodeposition, the modified electrode was dried at room temperature for 2 h. The ASA molecules were removed from the imprinted film by immersion the electrode in methanol-acetic acid (9:1, v/v) solution with stirring magnetically for 20 min.

2.6. Electroanalytical measurements

The electrochemical properties of the bare and modified electrodes were characterized using various electrochemical techniques including cyclic voltammetry (CV), electrochemical impedance spectroscopy (EIS) and square wave voltammetry (SWV). The rebinding of ASA molecules on the imprinted sensor was performed by incubating the modified electrode into a solution of ASA (pH 7.0) for 300 s with stirring. To characterize the MIP electrode, electrochemical measurements were carried out in a phosphate buffer solution (pH 7.0) containing 0.1 M KCl and 5.0 mM $K_3[Fe(CN)_6]/K_4[Fe(CN)_6]$ redox pair as a probe. The potential of CV was set from −0.10 to 0.50 V with a scan rate of 50 mV s^{-1}. Electrochemical impedance spectroscopy (EIS) was used at an applied potential of 0.20 V, amplitude of 10 mV and in a frequency range of 0.1–30,000 Hz. The square wave voltammograms (SWVs) were recorded under frequency of 15 Hz, amplitude of 20 mV and a step potential of 1 mV. All electrochemical measurements were conducted at room temperature.

2.7. Sample preparation

The tablet sample (80 mg acetylsalicylic acid tablet from Pars Darou Pharmaceutical Co., Tehran, Iran) was purchased from the local drug store. One tablet was accurately weighed and crushed into a powder and transferred to a 100 mL volumetric flask and dissolved in ethanol-distilled water solution (1:1 v/v) with shaking for 10 min in an ultrasonic bath. Then, the solution was filtered and diluted with phosphate buffer solution (pH 7.0) to the calibration line to obtain the required concentration for assay.

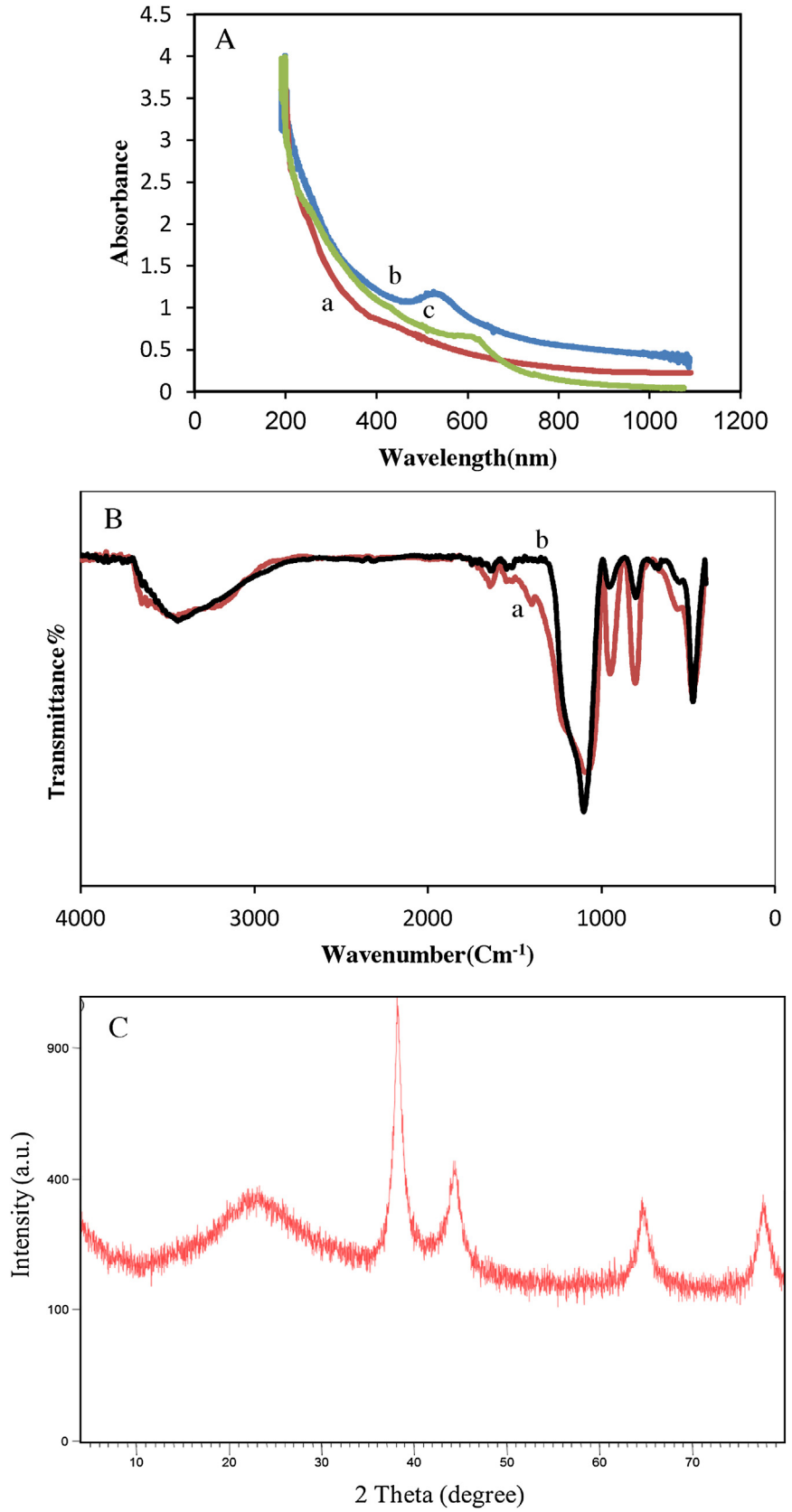

Fig. 2. A) UV–Vis spectra of (a) SiO_2, (b) Au and (c) SiO_2@AuNPs, B) FT-IR spectra of (a) SiO_2 and (b) SiO_2@AuNPs and C) XRD spectrum of SiO_2@AuNPs.

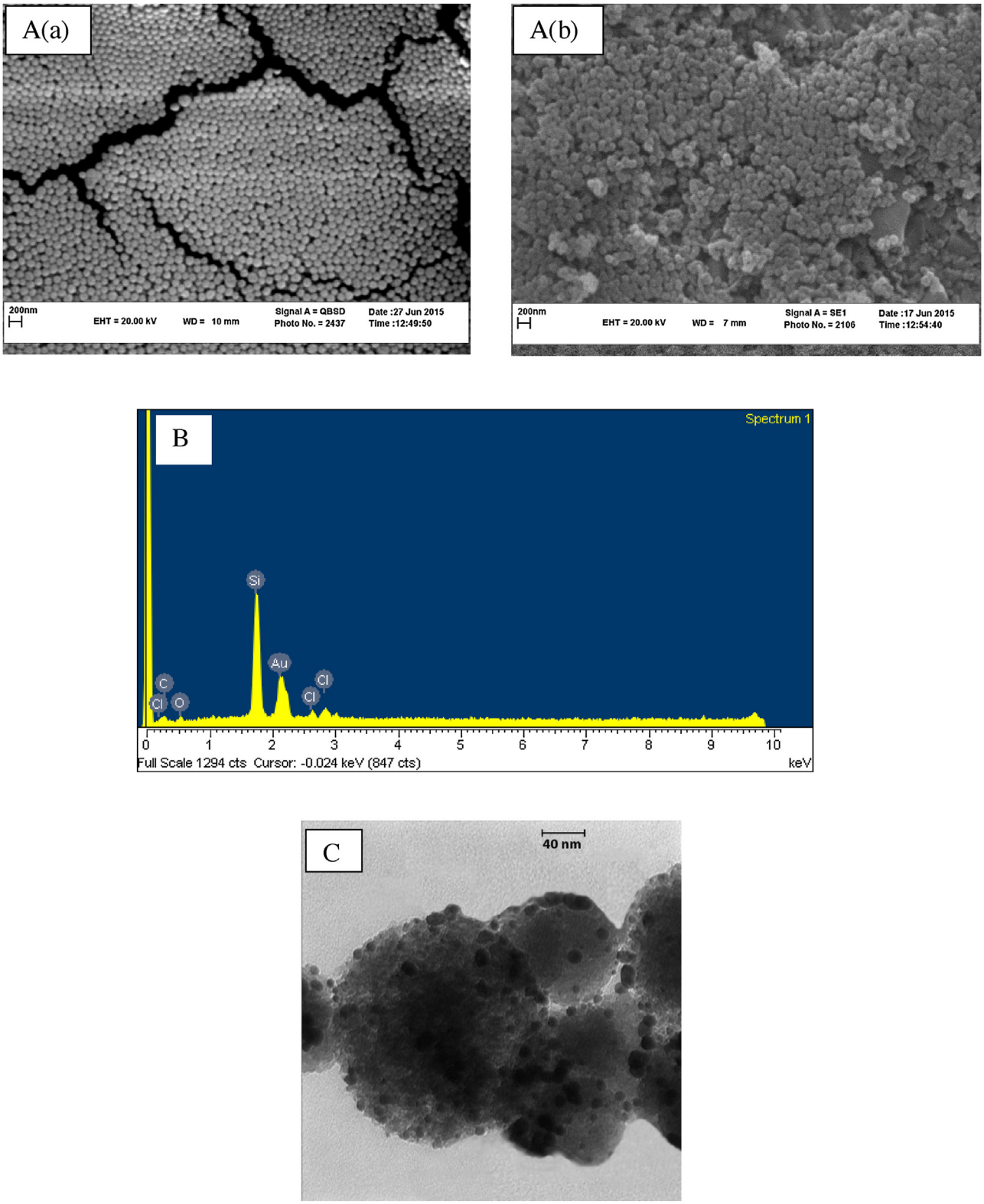

Fig. 3. A) Scanning electron microscope (SEM) images of (a) SiO_2, (b) SiO_2@AuNPs, B) EDX image of SiO_2@AuNPs and C) TEM image of SiO_2@AuNPs.

Drug-free human urine sample (taken from a healthy adult) was spiked with different concentrations of ASA. Prior to measurement, the sample was centrifuged for 10 min at 3500 rpm in order to remove the precipitated materials. Then, the supernatant was diluted (20-fold) with phosphate buffer solution (pH 7.0). Standard addition method was used for determination of ASA in the sample solutions.

3. Results and discussion

3.1. Characterization of the synthesized SiO_2@Au NPs

The spectra of UV–Vis, FT-IR and XRD pattern of SiO_2@AuNPs are shown in Fig. 2. Fig. 2A, shows the UV–Vis spectra of SiO_2, Au and SiO_2@AuNPs. The SiO_2@AuNPs absorption peak, demonstrates

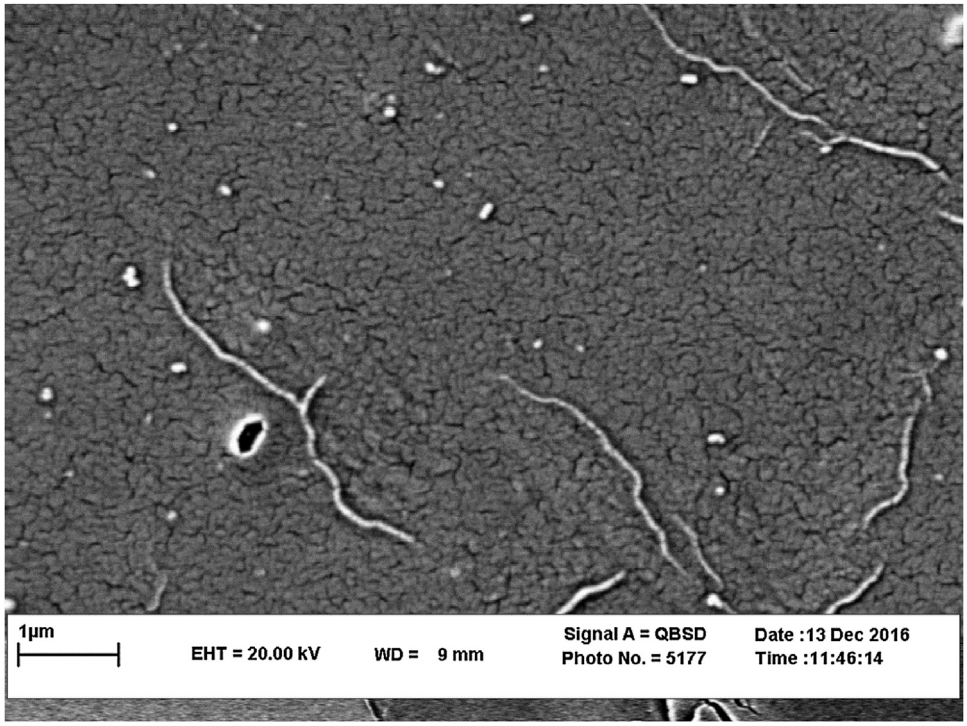

Fig. 4. Scanning electron microscope (SEM) image of polypyrrole/sol-gel/SiO_2@AuNPs MIP/Au electrode.

a broadening, decreasing the intensity and red shift from 524 to 615 nm which indicates that as more gold chloride molecules are reduced on the attached gold particles, their aspect ratio increases, which results in a red shift of the absorption peak. The mechanism for the broadening can be related to the extinction cross section and electron mean free path in the metal shell [32]. The FT-IR spectra of SiO_2 and SiO_2@AuNPs are shown in Fig. 2B. For SiO_2 and SiO_2@AuNPs, the peak at 1087 cm^{-1} can be assigned to asymmetric vibration of Si—O—Si bond, the peak at 805 cm^{-1} can be attributed to symmetric vibration of Si-O-Si bond and the peak at 950 cm^{-1} is assigned to asymmetric vibration of Si—OH bond. After coating the SiO_2 particles with the gold nanoparticles, the intensity of Si—O—Si and Si—OH peaks reduces significantly which confirms the successful formation of gold nanoshells onto the silica particles [25]. The XRD pattern of SiO_2@AuNPs is displayed in Fig. 2C. The crystalline structure of SiO_2@AuNPs is face centered cubic with the dominant crystal growth planes of (111). The silica shows a typical peak at 23°, and the peaks which are appeared at about 38.2°, 44.4°, 64.6° and 77.7° can be assigned to (111), (200), (220) and (311) crystalline plane diffraction peaks of gold.

The morphology, structure and composition of the SiO_2@AuNPs were investigated using scanning electron microscope (SEM), transmission electron microscope (TEM) and energy dispersive X-ray (EDX) analysis. The SEM images (Fig. 3A), show the uniformly prepared silica nanoparticles and also uniform attachment of the colloidal gold nanoparticles to the APTES-functionalized silica cores. The EDX analysis results (Fig. 3B), confirm the chemical composition of the prepared particles. Fig. 3C, illustrates the TEM image of SiO_2@AuNPs. As is shown in this Figure, the SiO_2 and SiO_2@AuNPs are nearly spherical and apparently well-dispersed. The diameter of SiO_2@AuNPs, was found to be in the range of 80 nm to 120 nm. The method used in this research work for fabrication of the SiO_2@AuNPs, has some benefits such as facile route, the same and spherical size for silica nanoparticles and also uniform attachment of the gold nanoparticles to the silica cores compared to the other methods for fabrication of SiO_2@AuNPs [33,34].

3.2. Preparation and characterization of imprinted sensor

The interaction design between the template molecule and functional monomers in the polymer matrix is crucial for optimizing the molecular imprinting process. The role of these functional monomers, is to form specific binding cavities in the imprinted film. The silane monomers which were used to prepare the imprinted sol-gel film, consisted of TEOS as the cross-linker to form a polymeric network around the template molecule through hydrogen bonds and ionic interactions, and PTEOS as the functional monomer for π–π interactions with the aromatic ring. Also, pyrrole was incorporated into the sol solution as an additional functional monomer to increase the stability of the resultant MIP. The —N—H group of the pyrrole units can also form hydrogen bonds with the C═O and the hydroxyl group of ASA molecules.

In the present work, the polypyrrole/sol-gel/SiO_2@AuNPs MIP sensor was fabricated by cyclic voltammetric (CV) method on the surface of Au electrode. During the electropolymerization, the ASA template molecules were diffused and trapped into the polymer matrix due to the interaction of ASA molecules with the functional monomers. The cyclic voltammograms of electropolymerization of imprinted film with and without ASA, didn't show any remarkable difference which reveals that ASA does not have any electrochemical behavior under the applied potential range for electrodepostion, and the structure of the ASA does not change during the imprinting process. The surface morphology of the nanocomposite film was investigated by scanning electron microscope (SEM). It can be seen from the SEM image (Fig. 4) that a layer of polypyrrole/sol-gel/SiO_2@AuNPs MIP has been attached to the surface of the gold electrode.

3.3. Electrochemical characterization of imprinted sensor

Cyclic voltammetry (CV) and electrochemical impedance spectroscopy (EIS) are effective and convenient techniques for monitoring the feature of the imprinted sensors. The cyclic voltam-

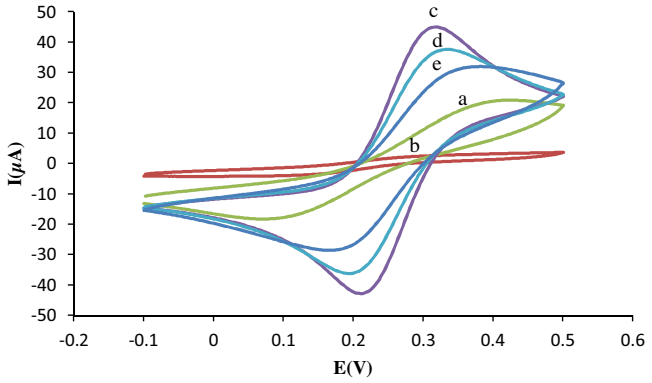

Fig. 5. Cyclic voltammograms (CVs) of (a) bare Au electrode, (b) MIP/Au electrode, (c) MIP/Au electrode after removal of ASA, (d) MIP/Au electrode after 300 s incubating in 5.0 nM ASA solution and (e) MIP/Au electrode without SiO_2@AuNPs after removal of ASA. Conditions: Potential scan range −0.1 V to +0.5 V, Scan rate 50 mV s^{-1}.

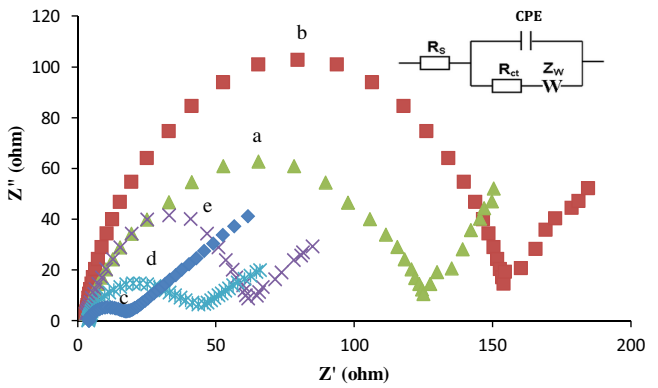

Fig. 6. Electrochemical impedance spectra (EIS) of (a) bare Au electrode, (b) MIP/Au electrode, (c) MIP/Au electrode after removal of ASA, (d) MIP/Au electrode after 300 s incubating in 5.0 nM ASA solution and (e) MIP/Au electrode without SiO_2@AuNPs after removal of ASA. Inset shows equivalent circuit model for impedance plots. Conditions: Potential 0.20 V, frequency range of 0.1–30000 Hz and at amplitude of 10 mV.

mograms of the bare and modified electrodes which were obtained in probe solution are shown in Fig. 5. At the bare Au electrode (curve 5a), a pair of redox peaks of $[Fe(CN)_6]^{3-/4-}$ are obtained. As can be seen in curve 4b, the current response of the electrode after electropolymerization of polypyrrole/sol-gel/SiO_2@AuNPs MIP is decreased significantly. Since the polymer film is coated on the surface of the electrode, the $[Fe(CN)_6]^{3-/4-}$ molecules cannot reach to the surface of the electrode and the electron transfer is blocked. After removal the template from the MIP film, the current response of the electrode increases (curve 5c). When the template is removed from the film, some channels are produced at the surface of the electrode which result in an increase the diffusion process of $[Fe(CN)_6]^{3-/4-}$ molecules through the imprinted polymer to the electrode surface. After the polypyrrole/sol-gel/SiO_2@AuNPs MIP/Au electrode is immersed in 5.0 nM ASA solution for 300 s, the current response of the sensor decreases (curve 5d). It seems that some of the cavities are recombined with ASA molecules which limit the chance for the electron transfer of the redox probe on the electrode surface. Also, after modification of the surface of the Au electrode with polypyrrole/sol-gel composite film (without SiO_2@AuNPs), the peak current decreases (curve 5e). To resolve this problem, the SiO_2@AuNPs were dispersed in the sol solution and entrapped within the polypyrrole/sol-gel composite film during electrodeposition process. The presence of SiO_2@AuNPs at the electrode surface, facilitates the electron transfer rate which may be due to the high conductivity and large specific surface area of the SiO_2@AuNPs.

Electrochemical impedance spectroscopy (EIS) can also be used to investigate the electrochemical properties of the surface of the modified electrodes. The impedance spectra include a semicircle portion and a linear portion. The semicircle diameter at higher frequencies corresponds to the electron-transfer resistance (R_{et}), and the linear part at lower frequencies is the characteristics of a diffusional limiting step of the electrochemical process. Fig. 6 shows the Nyquist diagrams of the modified electrode at different modification stages. The electrical equivalent circuit which was used for the analysis of EIS results is shown in the inset of Fig. 6. In this circuit, R_s, R_{et} and Z_w represent the resistance of electrolyte solution, electron-transfer resistance of the redox and Warburg impedance resulting from the diffusion of ions from the bulk of the electrolyte to the interface, respectively. A non-ideal frequency-dependent constant phase element (CPE) is instead of a pure capacitor to account for the effect of the roughness of electrode surfaces. CPE generates the impedance that can be expressed by the following relation [35]:

$$Z_{CPE}(\omega) = Z_0(j\omega)^{-\alpha} \quad (1)$$

where $0 < \alpha < 1$, j is the imaginary number, Z_0 is a constant, and ω is the angular frequency.

As can be seen in Fig. 6a, the bare Au electrode exhibits a semicircle part at high frequencies (R_{et} = 120.83 Ω) and a linear part at low frequencies. After the imprinted film is electrodeposited onto the Au electrode surface, the EIS displays an obvious increase in semicircle diameter (Fig. 6b), which indicates that the imprinted film, forms an additional barrier and the electron transfer of $[Fe(CN)_6]^{3-/4-}$ is blocked. When the template is removed from the surface of the electrode, the specific recognition sites which are formed on the MIP film, enhance the transfer rate of the $[Fe(CN)_6]^{3-/4-}$ probe (Fig. 6c). Furthermore, after immersing the polypyrrole/sol-gel/SiO_2@AuNPs MIP/Au electrode in 5.0 nM of ASA solution, the resistance increases, which can be attributed to the rebinding of template molecules into the imprinted sites which blocks the arrival of the $[Fe(CN)_6]^{3-/4-}$ probe onto the electrode surface.

3.4. Effect of different parameters on the sensor performance

In order to evaluate the performance of the constructed imprinted sensor, the effect of different influencing parameters such as scan cycles of electropolymerisation process, applied potential interval, amount of the monomers, template concentration, SiO_2@AuNPs percent, pH and the incubation time was investigated. The change in the current response of $[Fe(CN)_6]^{3-/4-}$ redox probe (Δi_p) was calculated by subtracting the current which resulted in the presence of ASA from the current recorded in the absence of ASA in solutions.

3.4.1. Electrodeposition conditions of MIP film

The number of electropolymerization cycle is a crucial factor in the preparation of MIP films, which can influence the thickness of the imprinted films. In the process of the electropolymerization, the number of scan cycles was varied from 3 to 12 for determination the optimal film thickness. The imprinted polymer films which were formed in less than 5 scan cycles, were found to be unstable and the higher numbers of the cycles led to the formation of a thick MIP film with less accessible imprinted sites [36]. Therefore, 5 scan cycles were used as the optimum number for construction of the designed electrode. In the electropolymerization step, different potential intervals were examined and the best response was obtained when the potential changed from −0.80 to +0.80 V.

3.4.2. Conditions of the sol solution

It is obvious that the composition and also the thickness of the coating layer at the surface of the electrode, have an important influence on its performance. For initial optimization of the composition of the sol solution, different polypyrrole/sol-gel/SiO_2@AuNPs MIP/Au electrodes were constructed by varying the amounts of TEOS and PTEOS in the sol solution, while their volume ratio was 1:1 and the final volume of the sol solution was kept constant. In addition, different imprinted sensors were fabricated by varying the pyrrole concentration in the range of 5.0–50.0 mM. The optimum amount was found to be: 150 μL of silane monomers (75 μL of TEOS and 75 μL of PTEOS) and 25.0 mM pyrrole monomer that were chosen to obtain the best performance. Below the optimum value of the functional monomers (TEOS, PTEOS, and pyrrole), the current decreases which may be due to lacking of enough imprinted sites and it seems that the ASA molecules cannot be captured during the electropolymerisation process. On the other hand, when the imprinted polymer film is too thick due to high concentration of monomers, the ASA molecules which are located at the central area of the polymer cannot be completely removed from the polymer network [37]. The effect of the amounts of template and SiO_2@Au core-shell nanoparticles was also investigated and it was found that 1.0 mM of the template and 1.5×10^{-3} percent (%W/V) of SiO_2@AuNPs are the most appropriate amounts for construction of the proposed sensor.

3.4.3. Rebinding conditions

The optimization of the incubation step is usually a simple and effective way to enhance the sensitivity of the imprinted sensor. After removing the template from the electrode surface, the imprinted sensor was incubated in a stirring 5.0 nM ASA solution containing phosphate buffer (pH 7.0) for different incubation times (Fig. 7A). As is evident in this Figure, the response current (Δi) increases with incubation time and reaches a platform at 300 s. Therefore, the incubation time of 300 s was selected for further studies.

It was found that the pH of the solution is effective on ASA rebinding at the surface of the modified electrode. Therefore, the effect of pH of ASA solution on the electrochemical response of the imprinted sensor was investigated in the pH range from 4.0 to 9.0 and the results are shown in Fig. 7B. As is evident in this Figure, the maximum current response is observed at pH 7.0, suggesting that this pH value can facilitate the interaction between the ASA molecules and the binding cavities. Therefore, the optimum pH of ASA solution was set at 7.0.

3.5. Selectivity of the MIP sensor

Selective recognition of a template molecule is an important parameter for a molecularly imprinted sensor. To evaluate the selectivity of the prepared MIP sensor, the salicylic acid, benzoic acid and carbolic acid (phenol) which have a similar structure to ASA were chosen as interfering species with an identical concentration. As is evident in Fig. 8, the current response of the MIP sensor is stronger than that of the NIP sensor, and the response of MIP sensor towards the ASA molecules is significantly higher than that towards the molecules of the structural analogs. This can be explained by the size, conformation and also the functional groups of the cavities that match ASA molecules in the imprinting film. Although the structures of the interfering species are relatively similar to ASA, their molecules cannot bind to the imprinted cavities as tightly as ASA molecules. Another factor for evaluation of the selectivity of the prepared sensor, is the imprinting factor (IF) which is defined as the ratio of the Δi_{MIP} to the Δi_{NIP}. As shown in Fig. 8, the IF value for ASA is 9.0 while in the case of interfering species it is in the range of 1.1–1.4. The results obtained in this study show that

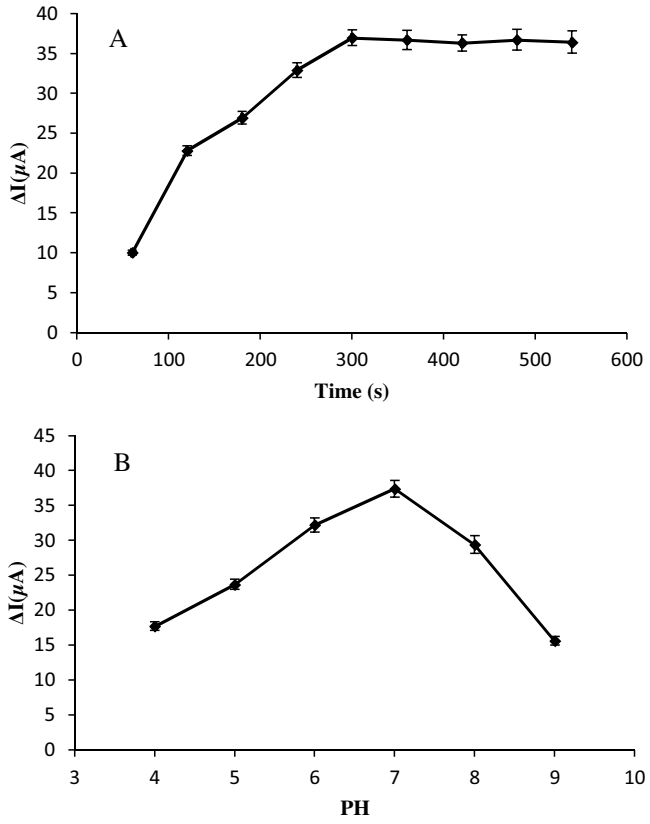

Fig. 7. Effect of (A) incubation time and (B) pH on the response current of the nanocomposite MIP sensor.

the proposed sensor exhibits a good selectivity towards the ASA molecules.

3.6. Analytical performance

The performance of the imprinted sensor for determination of ASA was investigated using square wave voltammetry technique under optimized experimental conditions. The inset of Fig. 9, shows the SWV responses of the polypyrrole/sol-gel/SiO_2@AuNPs MIP/Au electrode after incubation in the samples containing ASA at different concentrations for 300 s. Due to the occupation of the binding cavities in the imprinted film by ASA molecules, the peak current decreases as the concentration of ASA increases. As is shown in Fig. 9, two linear ranges from 1.0 to 10.0 nM and 10.0–100.0 nM for concentration of ASA are obtained with the regression equation of $\Delta i = 5.2234C + 12.861$ ($R^2 = 0.9971$) and $\Delta i = 0.289C + 63.0$ ($R^2 = 0.9959$), respectively, where C is ASA concentration (nM) and Δi is the current difference (μA). The limit of detection (LOD) was found to be 0.2 nM based on $3S_b/S$, where S and S_b represent the slope of the calibration curve and standard deviation of the blank (n = 5), respectively.

By using a methanol-acetic acid (9:1, v/v) binary solvent solution to remove the ASA molecules from the cavities, the imprinted sensor was able to be reused for 10 repeated analyses. The repeatability of one of the constructed electrochemical sensors was investigated for 5.0 nM ASA solution and the RSD was found to be: 3.0% (n = 10). Also, the fabrication reproducibility of the imprinted sensor was estimated by determination the response of 5.0 nM ASA solution using five fresh electrodes which were prepared independently under identical experimental conditions. The calculated RSD was about 3.8%. The stability of the MIP sensor was also studied on a two week period. The prepared sensor was stored at 4 °C and it

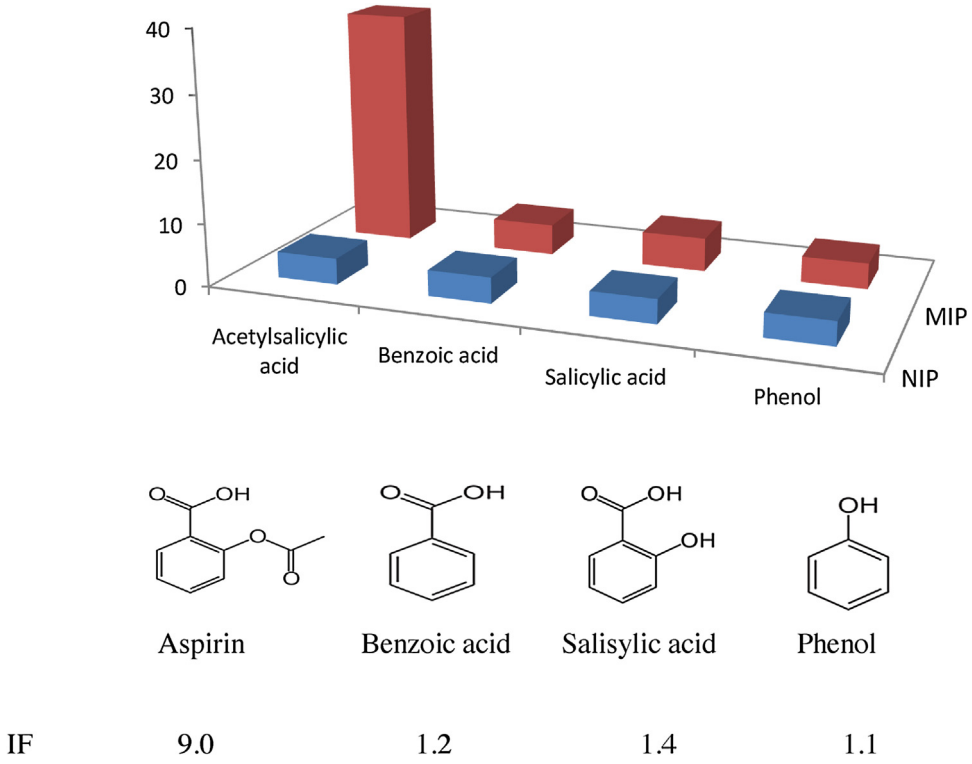

Fig. 8. Selectivity of the imprinted and non-imprinted sensor for acetylsalicylic acid and some interferences.

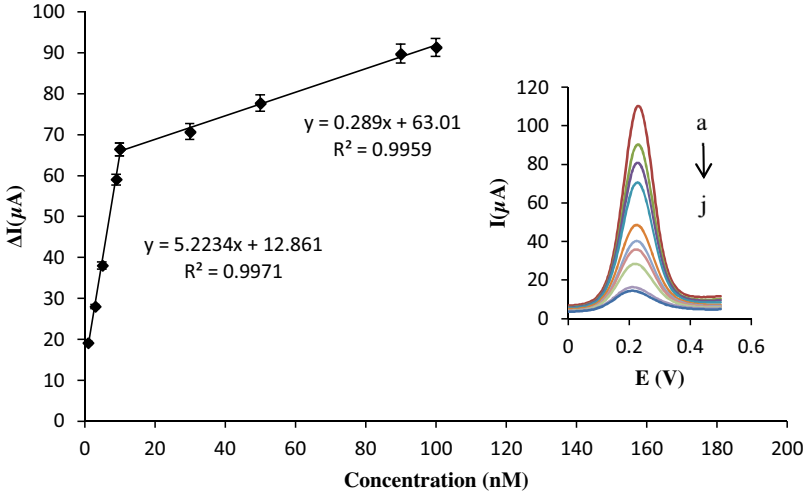

Fig. 9. Calibration curve of MIP sensor in different concentrations of ASA solutions. Error bars represent the standard deviations for three replicate measurements. Inset is the square wave voltammograms of polypyrrole/sol-gel/SiO_2@AuNPs MIP/Au electrode before (a) and after incubation in 1.0 (b), 3.0 (c), 5.0 (d), 9.0 (e), 10.0 (f), 30.0 (g), 50.0 (h), 90.0 (i) and 100.0 (j) nM of ASA solutions. Conditions: Potential scan range −0.1 V to +0.50 V, Step potential 1 mV, Frequency15 Hz, Amplitude, 20 mV in phosphate buffer pH 7.0 containing 0.1 M KCl and 1.0 mM $[Fe(CN)_6]^{3-/4-}$.

was used to detect the same ASA concentration every day. After two weeks, the sensor retained 91% of its initial response current, which demonstrates that the developed imprinted sensor has a good stability. The good stability of the MIP sensor may be due to the formation of a stiff layer of nanocomposite imprinted polymer on the surface of the electrode [38].

In order to verify the applicability of the proposed method, the prepared imprinted sensor was applied for determination of ASA in tablet and urine samples and the experimental results are summarized in Table 1. The samples were prepared by the procedures which are described in section 2.7. Each sample solution was spiked with appropriate amount of ASA. The standard addi-

Table 1
Results of acetylsalicylic acid determination in real samples (n = 3).

Sample	Added (nM)	Detected (nM)	(Recovery%)	(RSD%)
Tablet	–	4.8	–	4.2
	3.0	7.7	97	3.6
	5.0	10.1	106	3.4
	7.0	12.1	104	2.7
	10.0	14.6	98	2.5
Urine	–	Not detected	–	–
	3.0	3.1	103	3.2
	5.0	4.9	98	3.5
	7.0	7.3	104	2.7
	10.0	9.6	96	2.1

Table 2
Results obtained in the determination of ASA using the proposed and reference methods.

Sample	Lable value (mg)	Proposed method[a]	Reference method[a]	Relative error	
				RE1	RE_2
Tablet	80	78.6 ± 3.2	79 ± 2.9	−1.7	−0.5
Urine	80	78.3 ± 3.0	78.1 ± 3.3	−2.1	0.2

RE_1: [(proposed method value-label value)/label value] × 100.
RE_2: [(proposed method value- reference method value)/reference method value] × 100.
[a] Means ± s (n = 3).

Table 3
Comparison of some characteristics of the different electrodes for determination of acetylsalicylic acid in solutions.

Method	Linear range ($\mu mol\,L^{-1}$)	Detection limit ($\mu mol\,L^{-1}$)	Reference
NaMM/GCE	0.22–1.66	0.10	[40]
MWCNT–ACS/GCE	15.00–65.0	3.77	[41]
Surfactant–MWCNT/CPE	0.29–62.7	0.08	[10]
Bare EPPGE	0.02–100.0	0.01	[42]
GR-NF/GCE	0.87–17.0	6.5×10^{-2}	[43]
Polypyrrole/sol-gel/SiO_2@AuNPs MIP/Au	1×10^{-3}–0.1	2×10^{-4}	This work

NaMM/GCE: sodium montmorillonite modified glassy carbon electrode.
MWCNT–ACS/GCE: multiwalled carbon nanotube-alumina coated silica nanocomposite modified glassy carbon electrode.
EPPGE: edge plane pyrolytic graphite electrode.
GR-NF/GCE: graphene-nafion composite film modified glassy carbon electrode.

tion method was used for the analysis of the prepared samples. The acetylsalicylic acid content of the tablets which was declared by the manufacturer, was 80 mg per tablet; the acetylsalicylic acid content which was determined by the proposed sensor, was found to be: 78.6 mg per tablet. The proposed method was further validated by employing HPLC method as proposed in the Pharmacopoeia [39] and the results are given in Table 2. The obtained results, show that the values of recoveries and relative standard deviations (RSDs) are acceptable and the amounts of ASA which were determined by the proposed sensor, are in good agreement with the manufacturer's stated contents of ASA and the amounts obtained by the reference method, indicating that the constructed sensor response is not affected considerably by the sample matrix and the proposed method can be efficiently used for the determination of ASA in pharmaceutical and biological samples. The results obtained in this work and some of the previous procedures for determination of ASA are summarized in Table 3. Comparison of the summarized results in this Table 3, show that the present electrochemical sensor has a higher sensitivity with respect to the other constructed sensors for measurement the concentration of ASA in solutions.

4. Conclusion

In the present work, a simple approach was used to develop a novel electrochemical sensor for determination of acetylsalicylic acid (ASA) via one-step electropolymerization of nanocomposite molecularly imprinted polymer (MIP) on the surface of Au electrode. Under optimized experimental conditions, the proposed sensor displayed a good performance in terms of sensitivity, fast response, detection limit, stability, reproducibility and repeatability. The excellent performance of the polypyrrole/sol-gel/SiO_2@AuNPs modified electrode towards ASA molecules, can be attributed to the SiO_2@AuNPs with high conductivity and huge specific surface area and the porous imprinted nanocomposite film with plentiful selective recognition sites. Also, the prepared sensor exhibited a high recognition capacity towards the ASA molecules. The results obtained in this study, show that by using the conducting polymer (ppy), sol-gel technology and SiO_2@AuNPs for preparation of recognition elements, combined with electrochemical detection, we can determine ASA in pharmaceutical and biological samples successfully.

Acknowledgment

The authors gratefully acknowledge Ferdowsi University of Mashhad, Mashhad, Iran for supporting this work (Grant No. 3.32159).

Appendix A. Supplementary data

Supplementary data associated with this article can be found, in the online version, at http://dx.doi.org/10.1016/j.snb.2017.01.059.

References

[1] R.H. Böger, S.M. Bode-Böger, F.M. Gutzki, D. Tsikas, H.P. Weskott, J.C. Frölich, Rapid and selective inhibition of platelet aggregation and thromboxane formation by intravenous low dose aspirin in man, Clin. Sci. 84 (1993) 517–524.
[2] T.S. Poulsen, S.R. Kristensen, L. Korsholm, T. Haghfelt, B. Jørgensen, P.B. Licht, H. Mickley, Variation and importance of aspirin resistance in patients with known cardiovascular disease, Thromb. Res. 120 (2007) 477–484.
[3] T.J. Moore, M.J. Joseph, B.W. Allen, L.A. Coury, Enzymatically amplified voltammetric sensor for microliter sample volumes of salicylate, Anal. Chem. 67 (1995) 1896–1902.
[4] S.R. Polagani, N.R. Pilli, V. Gandu, High performance liquid chromatography mass spectrometric method for the simultaneous quantification of pravastatin and aspirin in human plasma: pharmacokinetic application, J. Pharm. Anal. 2 (2012) 206–213.
[5] M.S. Elmasry, I.S. Blagbrough, M.G. Rowan, H.M. Saleh, A.A. Kheir, P.J. Rogers, Quantitative HPLC analysis of mebeverine, mesalazine, sulphasalazine and dispersible aspirin stored in a Venalink monitored dosage system with co-prescribed medicines, J. Pharm. Biomed. Anal. 54 (2011) 646–652.
[6] M.J. Scotter, D.P.T. Roberts, L.A. Wilson, F.A.C. Howard, J. Davis, N. Mansell, Free salicylic acid and acetyl salicylic acid content of foods using gas chromatography-mass spectrometry, Food Chem. 105 (2007) 273–279.
[7] R. Szostak, S. Mazurek, Quantitative determination of acetylsalicylic acid and acetaminophen in tablets by FT-Raman spectroscopy, Analyst 127 (2002) 144–148.
[8] M.O. Iwunze, Absorptiometric determination of acetylsalicylic acid in aqueous ethanolic solution, Anal. Lett. 41 (2008) 2944–2953.
[9] A.B. Moreira, I.L.T. Dias, G.O. Neto, E.A.G. Zagattoc, M.M.C. Ferreira, L.T. Kubota, Solid-phase spectrofluorimetric determination of acetylsalicylic acid and caffeine in pharmaceutical preparations using partial least-squares multivariate calibration, Talanta 67 (2005) 65–69.
[10] B.J. Sanghavi, A.K. Srivastava, Simultaneous voltammetric determination of acetaminophen, aspirin and caffeine using an in situ surfactant-modified multiwalled carbon nanotube paste electrode, Electrochim. Acta 55 (2010) 8638–8648.
[11] E.R. Sartori, R.A. Medeiros, R.C. Rocha-Filho, O. Fatibello-Filho, Square-wave voltammetric determination of acetylsalicylic acid in pharmaceutical formulations using a boron-doped diamond electrode without the need of previous alkaline hydrolysis step, J. Braz. Chem. Soc. 20 (2009) 360–366.
[12] X. Jiang, C. Zhao, N. Jiang, H. Zhang, M. Liu, Selective solid-phase extraction using molecular imprinted polymer for the analysis of diethylstilbestrol, Food Chem. 108 (2008) 1061–1067.
[13] M. Ahmadi Golsefidi, Z. Es'haghi, A. Sarafraz-Yazdi, Design, synthesis and evaluation of a molecularly imprinted polymer for hollow fiber-solid phase microextraction of chlorogenic acid in medicinal plants, J. Chromatogr. A 1229 (2012) 24–29.
[14] Y.L. Wang, Y.L. Gao, P.P. Wang, H. Shang, S.Y. Pan, X.J. Li, Sol–gel molecularly imprinted polymer for selective solid phase microextraction of organophosphorous pesticides, Talanta 115 (2013) 920–927.
[15] N. Karimian, M. Vagin, M.H. Arbab Zavar, M. Chamsaz, A.P.F. Turner, A. Tiwari, An ultrasensitive molecularly-imprinted human cardiac troponin sensor, Biosens. Bioelectron. 50 (2013) 492–498.
[16] D. Zang, M. Yan, S. Ge, L. Ge, J. Yu, A disposable simultaneous electrochemical sensor array based on a molecularly imprinted film at a NH_2-graphene modified screen-printed electrode for determination of psychotropic drugs, Analyst 138 (2013) 2704–2711.
[17] A. Afkhami, H. Ghaedi, T. Madrakian, M. Ahmadi, H. Mahmood-Kashani, Fabrication of a new electrochemical sensor based on a new nano-molecularly imprinted polymer for highly selective and sensitive determination of tramadol in human urine samples, Biosens. Bioelectron. 44 (2013) 34–40.

[18] J. Li, Z. Chen, Y. Li, A strategy for constructing sensitive and renewable molecularly imprinted electrochemical sensors for melamine detection, Anal. Chim. Acta 706 (2011) 255–260.
[19] B. Rezaei, H. Lotfi-Forushani, A.A. Ensafi, Modified Au nanoparticles-imprinted sol-gel, multiwall carbon nanotubes pencil graphite electrode used as a sensor for ranitidine determination, Mater. Sci. Eng. C 37 (2014) 113–119.
[20] A. Olwill, H. Hughes, M. O'Riordain, P. McLoughlin, The use of molecularly imprinted sol-gels in pharmaceutical separations, Biosens. Bioelectron. 20 (2004) 1045–1050.
[21] Z. Zhang, Y. Hu, H. Zhang, L. Luo, S. Yao, Layer-by-layer assembly sensitive electrochemical sensor for selectively probing L-histidine based on molecular imprinting sol–gel at functionalized indium tinoxide electrode, Biosens. Bioelectron. 26 (2010) 696–702.
[22] A. Geto, M. Tessema, S. Admassie, Determination of histamine in fish muscle at multi-walled carbon nanotubes coated conducting polymer modified glassy carbon electrode, Synth. Met. 191 (2014) 135–140.
[23] X. Kan, H. Zhou, C. Li, A. Zhu, Z. Xing, Z. Zhao, Imprinted electrochemical sensor for dopamine recognition and determination based on a carbon nanotube/polypyrrole film, Electrochim. Acta 63 (2012) 69–75.
[24] A. Mehdinia, M.O. Aziz-Zanjani, M. Ahmadifar, A. Jabbari, Design and synthesis of molecularly imprinted polypyrrole based on nanoreactor SBA-15 for recognition of ascorbic acid, Biosens. Bioelectron. 39 (2013) 88–93.
[25] M. Kazemzadeh Otoufi, N. Shahtahmasebi, A. Kompany, E. Kafshdar Goharshadi, A. Roghani, gradual growth of gold nanoseeds on silica for silica@gold core–shell nano applications by two different methods: a comparison on structural properties, J. Clust. Sci. 25 (2014) 1307–1317.
[26] S. Guo, E. Wang, Synthesis and electrochemical applications of gold nanoparticles, Anal. Chim. Acta 598 (2007) 181–192.
[27] M.H. Rashid, R.R. Bhattacharjee, A. Kotal, T.K. Mandal, Synthesis of spongy gold nanocrystals with pronounced catalytic activities, Langmuir 22 (2006) 7141–7143.
[28] D. Yu, Y. Zeng, Y. Qi, T. Zhou, G. Shi, A novel electrochemical sensor for determination of dopamine based on AuNPs@SiO_2 core-shell imprinted composite, Biosens. Bioelectron. 38 (2012) 270–277.
[29] A. Afkhami, A. Shirzadmehr, T. Madrakian, H. Bagheri, Improvement in the performance of a Pb^{2+} selective potentiometric sensor using modified core/shell SiO_2/Fe_3O_4 nano-structure, J. Mol. Liq. 199 (2014) 108–114.
[30] Y. Hu, J. Li, Z. Zhang, H. Zhang, L. Luo, S. Yao, Imprinted sol–gel electrochemical sensor for the determination of benzylpenicillin based on Fe_3O_4@SiO_2/multi-walled carbon nanotubes-chitosans nanocomposite film modified carbon electrode, Anal. Chim. Acta 698 (2011) 61–68.
[31] W. Stöber, A. Fink, E. Bohn, Controlled growth of monodisperse silica spheres in the micron size range, J. Colloid Interface Sci. 26 (1968) 62–69.
[32] J. Park, A. Estrada, K. Sharp, K. Sang, J.A. Schwartz, D.K. Smith, C. Coleman, J.D. Payne, B.A. Korgel, A.K. Dunn, J.W. Tunnell, Two-photon-induced photoluminescence imaging of tumors using near-infrared excited gold nanoshells, Opt. Express 16 (2008) 1590–1599.
[33] D. Kandpal, S. Kalele, S.K. Kulkarnl, Synthesis and characterization of silica – gold core-shell (SiO_2 @Au) nanoparticles, Pramana, J. Phys. 69 (2007) 277–283.
[34] S.L. Westcott, S.J. Oldenburg, T.R. Lee, N.J. Halas, Formation and adsorption of clusters of gold nanoparticles onto functionalized silica nanoparticle surfaces, Langmuir 14 (1998) 5396–5401.
[35] J. Bisquert, G. Garcia-Belmonte, P. Bueno, E. Longo, L.O.S. Bulho˜es, Impedance of constant phase element (CPE)-blocked diffusion in film electrodes, J. Electroanal. Chem. 452 (1998) 229–234.
[36] W. Lian, S. Liu, J. Yu, J. Li, M. Cui, W. Xu, J. Huang, Electrochemical sensor using neomycin-imprinted film as recognition element based on chitosan-silver nanoparticles/graphene-multiwalled carbon nanotubes composites modified electrode, Biosens. Bioelectron. 44 (2013) 70–76.
[37] B.L. Li, J.H. Luo, H.Q. Luo, N.B. Li, A novel strategy for selective determination of d-penicillamine based on molecularly imprinted polypyrrole electrode via the electrochemical oxidation with ferrocyanide, Sens. Actuators B 186 (2013) 96–102.
[38] B. Rezaei, M. Khalili Boroujeni, A.A. Ensafi, A novel electrochemical nanocomposite imprinted sensor for the determination of lorazepam based on modified polypyrrole@sol-gel@gold nanoparticles/pencil graphite electrode, Electrochim. Acta 123 (2014) 332–339.
[39] United States Pharmacopoeia XXII US Pharmacopeial Convention, Rockville MD 1990 113.
[40] B. Muralidharan, G. Gopu, C. Vedhi, P. Manisankar, Voltammetric determination of analgesics using a montmorillonite modified electrode, Appl. Clay Sci. 42 (2008) 206–213.
[41] T.L. Lu, Y.C. Tsai, Electrocatalytic oxidation of acetylsalicylic acid at multiwalled carbon nanotube-alumina-coated silica nanocomposite modified glassy carbon electrodes, Sens. Actuators B 148 (2010) 590–594.
[42] R.N. Goyal, S. Bishnoi, B. Agrawal, Electrochemical sensor for the simultaneous determination of caffeine and aspirin in human urine samples, J. Electroanal. Chem. 655 (2011) 97–102.
[43] A. Yiğit, Y. Yardım, M. Çelebi, A. Levent, Z. Şentürk, Graphene/Nafion composite film modified glassy carbon electrode for simultaneous determination of paracetamol, aspirin and caffeine in pharmaceutical formulations, Talanta 158 (2016) 21–29.

Biographies

Behjat Deiminiat is a Ph.D. student of Analytical Chemistry at Ferdowsi University of Mashhad, Mashhad, Iran. She received her M.Sc. degree in Analytical Chemistry from the same university in 2010. Her research interests include the development of electrochemical sensors based on molecularly imprinted polymers and aptasensors.

Iman Razavipanah (born Mashhad, Iran, 1982) received his B.Sc., M.Sc. and Ph.D. degrees from Ferdowsi University of Mashhad, in Mashhad (Iran). His research is focused on the development of electrochemical sensors, synthesis of electrocatalysts and photoelectrocatalysts for fuel cells and new electrochemically prepared SPME coatings. He has published more than 40 peer-reviewed and conference papers on these topics.

Gholam Hossein Rounaghi is a full distinguished professor of Chemistry at Ferdowsi University of Mashhad, Mashhad, Iran. He received his B.Sc. degree in Chemistry from Ferdowsi University of Mashhad, in 1970, his M.Sc. degree in Analytical Chemistry at the same university in 1973, and his PhD degree from Michigan State University (MSU) in Analytical Chemistry in 1980. His research interests focus on the study of complexation of macrocyclic ligands with metal cations in non-aqueous solvents and development of electrochemical sensors for cations and pharmaceutical compounds.

Mohammad Hossein Arbab-Zavar is a full distinguished professor of Chemistry at Ferdowsi University of Mashhad, Mashhad, Iran. He was graduated in Chemistry (B.Sc. degree) from Shahid Beheshti University, Tehran, (Iran) in 1968 and then he received M.Sc. and Ph.D. in Analytical Chemistry from University of Southampton (England) in 1978 and 1982, respectively. His research interests include electrochemical hydride generation for measurement of some toxic elements and development of electrochemical sensors and their application in electrochemical analysis.